



## Computer-based grading of haematoxylin-eosin stained tissue sections of urinary bladder carcinomas

P. SPYRIDONOS†, P. RAVAZOULA‡, D. CAVOURAS§,  
K. BERBERIDIS¶ and G. NIKIFORIDIS\*†

†Computer Laboratory, School of Medicine, University of Patras, Rio, Patras 265 00, Greece

‡Department of Pathology, University Hospital, Rio, Patras 265 00, Greece

§Department of Medical Instrumentation Technology, Technological Education Institution of Athens, Ag. Spyridonos Street, Aigaleo, 122 10 Athens, Greece

¶Department of Computer Engineering and Informatics, School of Engineering, University of Patras, Rio, Patras 265 00, Greece

**Abstract.** *Purpose:* A computer-based image analysis system was developed for assessing the malignancy of urinary bladder carcinomas in a more objective manner. Tumours characterized in accordance with the WHO grading system were classified into low-risk (grades I and II) and high-risk (grades III and IV).

*Materials and methods:* Images from 92 haematoxylin-eosin stained sections of urinary bladder carcinomas were digitized and analysed. An adequate number of nuclei were segmented from each image for morphologic and textural analysis. Image segmentation was performed by an efficient algorithm, which used pattern recognition methods to automatically characterize image pixels as nucleus or background. Image classification into low-risk or high-risk tumours was performed by means of the quadratic non-linear Bayesian classifier, which was designed employing 36 textural and morphological features of the nucleus.

*Results:* Automatic segmentation of nuclei on all images was about 90% on average. Overall system accuracy in correctly classifying tumours into low-risk or high-risk was 88%, employing the leave-one-out method and the best combination of three textural and one morphological feature. Classification accuracy for low-risk tumours was 88.8% and for high-risk tumours 86.2%.

*Conclusion:* The proposed image analysis system may be of value to the objective assessment of the malignancy of urine bladder carcinomas, since it relies on nuclear parameters that are employed in visual grading and their prognostic value has been proved.

*Keywords:* Computer-based classification; Grading of bladder carcinoma; nuclei morphometry; Multivariate statistical methods.

### 1. Introduction

Grading histological sections of urinary bladder tumours is used for cancer prognosis and consequently the choice of treatment is highly dependent on it [1]. Tumours characterized by the World Health Organization (WHO) grading system [2] are classified into low-grade and high-grade [3]. Low-grade tumours are less

\*Author for correspondence; e-mail: gnikif@med.upatras.gr

aggressive and are less likely to grow or spread and they encompass tumours of grade I or II. Tumours of grade III or IV are assigned high-grade. Grading performed by a pathologist incorporates various tissue, cell, and nuclear characteristics, which are assumed to be correlated to the degree of malignancy [4]. Thus, the final decision about the tumour is highly subjective [5]. Especially for intermediate tumours of grade II, which seem to be a continuum between grades I and III, the inter- and intra-observer reproducibility is low. From a clinical point of view it is important to distinguish low-grade tumours, which can generally be treated conservatively in contrast to high-grade tumours. The latter often require a more aggressive therapy because of a high-risk cancer progression [6]. Hence, there is a need for the development of reliable and reproducible systems for assessing tumour aggressiveness. Several approaches using computer-based methods have attempted to quantitate the malignancy of cancer in a more objective manner [7–11].

Previous studies on computer-based automatic classification of bladder carcinoma [9, 10] have used in the design of their systems a modification to the WHO grading system, using I, IIA, IIB, III tumour grading [12]. They have relied on tissue characteristics, relational or textural, rather than individual nuclear features. However, as recent studies [13–16] have revealed, features concerning the morphology or texture of the nucleus could provide significant prognostic information.

In the present study, we have developed a computer-based image analysis system for the automatic characterization of bladder carcinoma as high risk (grades III and IV) or low risk (grades I and II), employing the WHO grading system and morphological and textural features of the nucleus.

## 2. Materials and methods

The Department of Pathology of the University Hospital of Patras, Greece, has provided the haematoxylin-eosin (HE) stained paraffin tissue sections of 92 patients (cases) with urine bladder carcinoma used in the present study. All cases had been characterized by four independent pathologists using the WHO grading system, and sixty-three cases had been classified as low grade and 29 as high grade. Images (fields) of tissue specimens were captured using a light microscopy imaging system consisting of a Zeiss KF2 microscope and an Ikegami colour video camera. From each case up to three randomly selected fields were captured at a magnification of X400 from a region predefined by the pathologists. Additionally, each digitized image ( $768 \times 576 \times 24$ -bit resolution) was converted into an 8-bit grey scale image for further processing and analysis.

### 2.1. Image segmentation

An adequate number of nuclei were segmented from each case of morphologic and texture analysis. For image segmentation, an efficient algorithm based on the principle of minimum distance was developed as follows. From each bladder image, a large number of small  $5 \times 5$  pixel image samples from the nucleus and from the surrounding nucleus texture (background) were selected, thus forming two distinct classes: nucleus and non-nucleus image samples. Two textural features from the auto-correlation function [17] (Appendix A, equations A6–7) were evaluated from each image sample, which were then employed in the design of a minimum distance decision rule. Segmentation was then performed by

scanning each image by a  $5 \times 5$  pixel mask and characterizing each image pixel as nucleus or background, on the basis of local textural evaluations and distances from the representative means (Appendix A, equation A1). In this way, each bladder image was transformed into a nucleus-image by retaining only those pixels belonging to the nucleus class. In the case of misclassification (about 10% of the nuclei) due to nucleus overlapping, suitable morphological filters (Appendix A, equations A8–9) were employed for nucleus delineation or morphological features were used for nucleus rejection.

## 2.2. Feature generation

For each case at least 30 nuclei (Appendix C) were extracted, from one or more fields, in order to be employed in the design of the image analysis system. For each nucleus 36 morphological and textural features were evaluated. Morphological features consisted of nucleus area, roundness, and concavity [18]. Textural features included mean value, variance, skewness, and kurtosis from the nucleus intensity histogram, and the rest were computed from the co-occurrence matrix [19–22], which is a two-dimensional histogram describing the frequency with which two adjacent pixels occur in the nucleus's image. Finally, each one of the 92 cases was represented by a 36 feature vector, each feature being forms as the mean feature of all nuclei evaluated in each case.

## 2.3. Feature selection and classification

Best features selection was based on the performance of the classifier. Features were combined in all possible ways (i.e. 2, 3, 4, 5 feature combinations) by the Bayesian classifier [23] (Appendix C, equation C1) in order to determine the highest classification accuracy achieved with the minimum number of features [24] (Appendix B).

Classifier performance evaluation was tested by means of the leave-one-out method [25], and the results were presented in a truth table, revealing the classification accuracy of the system.

## 3. Results

Each greyscale image was automatically segmented into nuclei and background and at least 30 nuclei were extracted from each case. Since the number of accurate segmented nuclei per section field ranged approximately between 17 and 65, two fields were mostly sampled in each case. Only one case of grade IV required more than 3 fields. In all cases, nuclei were located with an overall accuracy of about 90%. Figures 1 and 2 show samples of bladder carcinoma and figures 3 and 4 show the results of the segmentation algorithm.

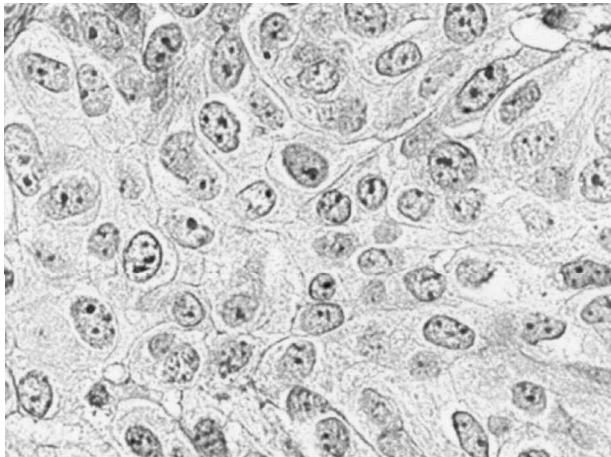
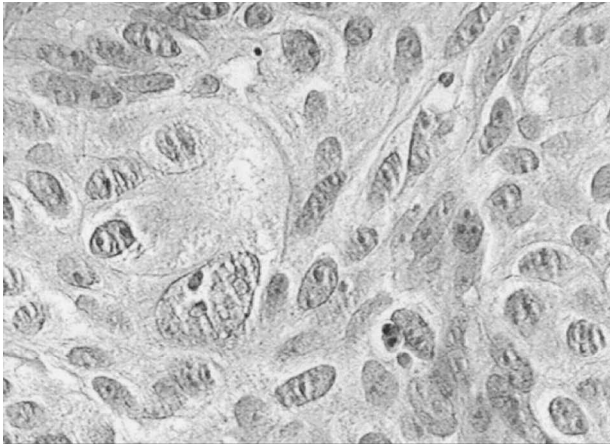
The best classification result was obtained in four-dimension feature space. The overall classification accuracy was 88%, employing the variance of nucleus histogram, the texture feature correlation for  $d = 1$  and  $d = 3$ , and the standard deviation of concavity (Appendix B).

As shown in table 1, 88.8% (56/63) of the low-risk cases were correctly classified while 7 cases were misclassified as high-risk. This false positive finding (11%) concerned only grade II tumours. In the high-risk group the correct classification was 86.2% (25/29) and four cases were misclassified as low-risk tumours. This false negative finding (13.7%) concerned grade III tumours.

#### 4. Discussion

Subjective assessment in pathologic diagnosis may be influenced by various factors including the reproducibility of some grading systems, which can be as low as 30–40% [26, 27], on the psycho-physiological performance of the diagnostician [28], and on the quality of the definition of each category. Particular problems may arise in distinguishing grade II and grade III tumours [29], which may characterize a tumour as of low or high risk. Some research workers [10] have developed image perception techniques instead of subjectively characterizing tumours. Other studies [30, 31] have attempted to assist pathologic diagnosis by introducing computer-aided image analysis methods during the last 32 years. Such methods have claimed a more objective and reproducible manner in urinary bladder carcinoma prognosis [7, 15].

The aim of this study was to develop an automatic image analysis method for characterizing urinary bladder carcinomas as low-risk tumours (grades I and II) or high-risk tumours (grades III and IV). In contrast to previous studies [9, 10],



Figures 1 and 2. Samples of bladder carcinoma.

it has been our objective from the beginning to rely on the WHO grading system, which is widely adopted by pathologists, and to employ morphological and textural features of the nucleus, since such parameters are used in visual grading and their prognostic value has been proved [13–16]. In this way our method would be closely associated to the work performed by the pathologist.

Locating the nuclei from their background on each field is a difficult task that has been mainly dealt with thresholding techniques. Previous studies [9, 10] have used global thresholding techniques for the initial labeling of nuclei regions. However, in our case image intensity properties of HE stained sections varied widely and the internal part of nuclei was very heterogeneous to adapt a similar method. Our segmentation method relied on a different approach, that of applying pattern recognition methods in characterizing image pixels as belonging to nucleus or to background (figures 1–4). Segmentation results on all images of the present study revealed a high percentage (about 90%) accuracy in automatic delineation of all image nuclei. The method was fast, reproducible, and without operator bias.

The quadratic non-linear Bayesian classifier was trained to classify a set of 92 cases in two classes according to the degree of malignacy. Each case was defined by 36 parameters, comprising only morphological and textural nucleus features. Previous studies [9, 10] have relied on linear discriminant classification techniques, which however are less sensitive to wide pattern clustering. The overall classification accuracy of the image analysis system that we have developed was 88% in distinguishing high-risk from low-risk bladder carcinomas. The results appear encouraging considering that they have been obtained by using only textural and morphological parameters of the nucleus, which may contain important information on the nature as well as the progression or recurrence of the disease. Additionally, grading based on HE stained sections is a widely used method adopted in everyday practice by many laboratories and our intention has been to develop a diagnostic tool for that grading procedure. Previous studies on computer-aided classification of urinary bladder carcinoma [9, 10] have relied on different features with no particular focus on the nucleus, have employed a different tumour subjective grading system (modified WHO grading), and have used a different tissue section staining procedure.

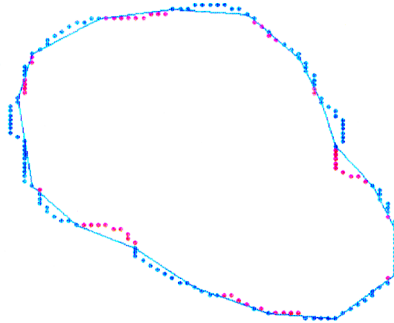
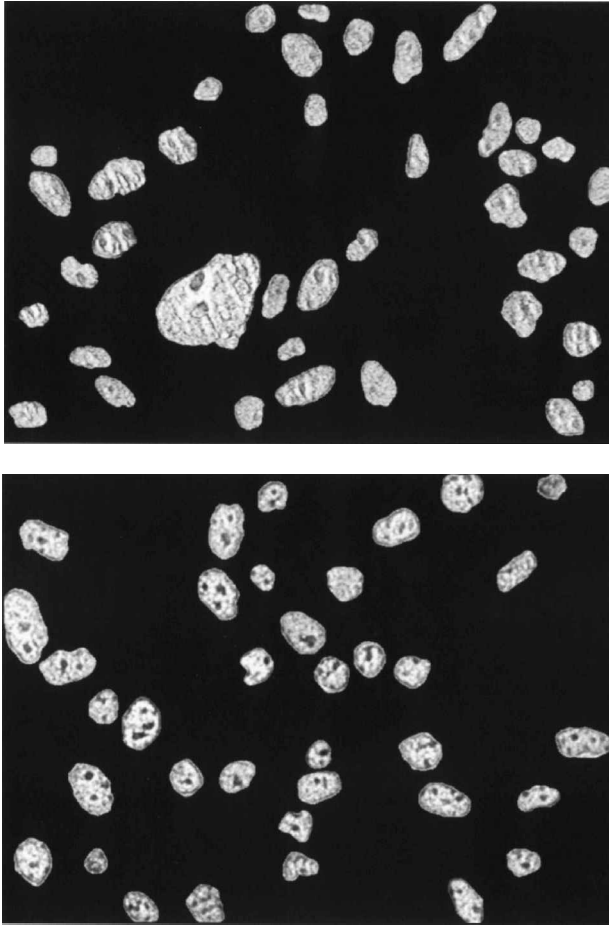


Figure B1. An arbitrary position of the chords on the nuclear contour. For this particular nucleus 39 different chord positions will give the mean value of concavity.



Figures 3 and 4. Processed images displaying clearly the segmented nuclei.

Table 1. Truth table demonstrating system classification of 92 bladder carcinoma cases into low-risk (grades I or II) and high-risk (grades III or IV).

Pathological finding	System classification		Accuracy
	Low-risk	High-risk	
Low-risk	56	7	88.8%
High-risk	4	25	86.2%
Overall accuracy			88%

The classification accuracy for the low-risk tumours was 88.8%. Considering that in the low-risk class we have included all grade II tumours, results are very satisfactory since grade II is a confusing category signifying the continuum between grade I and grade III [8, 11]. This may be also verified in our results, since all seven misclassified tumours have been characterized as grade II. Perhaps this is the reason that has led previous studies to adopting a modified

WHO grading system, by splitting grade II tumours into the low-risk and high-risk groups. Regarding the high-risk tumour classification accuracy, 86.2% of the tumours were correctly classified, while four (13.7%) grade III tumours were wrongly characterized as low-risk. The importance of this result may be assessed by considering that the burden for low-grading a tumour may be decisive in patient management and, thus, in the progression or recurrence of the disease. Therefore, it was important to employ textural and morphological features of the nucleus for estimating tumour grading, because of their high prognostic value.

Regarding the nuclear features used for achieving the highest classification accuracy, the best combination consisted of three textural features and one morphological feature (Appendix B). The variance of the nucleus intensity (Appendix B, equation B1) signifies the inhomogeneity of the chromatin texture of the nucleus [11], the correlation (Appendix B, equation B4) signifies grey-tone linear dependencies in the nucleus image [20], and the concavity is the morphological descriptor sensing slight irregularities in the nucleus borders.

In conclusion, an automatic image analysis method has been developed for characterizing urinary bladder carcinomas as low-risk tumours (grades I and II) or high-risk tumours (grades III and IV), based on textural and morphological features of the nucleus and on the WHO grading system. The usefulness of the system is its ability to automatically segment the nuclei on digitized tissue sections, following the widely used HE tissue-section staining procedure, and to provide diagnostic information with high accuracy.

## References

1. COLLAN, Y., MAKINEN, J. and HEIKKINEN, A., 1979, Histological grading to TC tumors of the bladder. Value of histological grading (WHO) in prognosis. *European Urology*, 5-311.
2. JONATHAN, I. E., MAHUL, B. A., VICTOR, R. R. and MOSTOFI, F. K., 1998, The World Health Organization/International Society of Urological Pathology consensus classification of urothelial (transitional cell) neoplasms of the urinary bladder. *American Journal of Surgical Pathology*, 22, 1435-1448.
3. MURPHY, W. M., 1989, Diseases of the urinary bladder, urethra, ureters, and renal pelves. In *Urological pathology*, edited by W. M. Murphy (Philadelphia: WB Saunders), 64-96.
4. BUSCH, C., ENGBERG, A., NORLEN, B. J. and STENKVIST, B., 1977, Malignancy grading of epithelial bladder tumors. *Scandinavian Journal of Urology and Nephrology*, 11, 143-148.
5. OOMS, E. C. M., KURVER, P. H. J., VELDTHUIZEN, R. W. and ALONS, C. L., 1983, Morphometric grading of bladder tumours in comparison with histologic grading by pathologists. *Human Pathology*, 14, 140-143.
6. MALMSTROM, P.-U., BUSCH, C. and NORLEN, B. J., 1987, Recurrence, progression and survival in bladder cancer. *Scandinavian Journal of Urology and Nephrology*, 21, 185-195.
7. PREWITT, J. M. S., 1978, On some applications of pattern recognition and image processing to cytology, cytogenetics and histology. Doctoral dissertation, Department of Computer Science and Department of Clinical Cytology, Uppsala University.
8. DE MEESTER, U., YOUNG, I. T., LINDEMAN, J. and VAN DER LINDEN, H. C., 1991, Towards a quantitative grading of bladder tumors. *Cytometry*, 12, 602-613.
9. JARKRANS, T., VASKO, J., BENGTSOON, E., CHOI, H.-K., MALMSTROM, P.-U., WESTER, K. and BUSCH, C., 1995, Grading of transitional cell bladder carcinoma by image analysis of histological sections. *Analytical Cellular Pathology*, 18, 135-138.
10. CHOI, H.-K., VASKO, J., BENGTSOON, E., JARKRANS, T., MALMSTROM, P.-U., WESTER, K. and BUSCH, C., 1994, Grading of transitional cell bladder carcinoma by texture analysis of histological sections. *Analytical Cellular Pathology*, 6, 327-343.

11. VAN VELTHOVEN, R., PETEIN, M., ZLOTTA, A., OOSTERLINCK, W., MEIJDEN, A., ZANDONA, C., ROELS, H., PASTELS, J. L., SCHULMAN, C., and KISS, R. 1994, Computer-assisted chromatin texture characterization of Feulgen-stained nuclei in a series of 331 transitional bladder cell carcinomas. *Journal of Pathology*, **173**, 235–242.
12. PAUWELS, R. P. E., SCHAPERS, R. F. M., SMEETS, A. W. G. B., DEBRUYNE, F. M. J. and GARAEDTS, J. P. M., 1988, Grading in superficial bladder cancer: (1) morphological criteria. *British Journal of Urology*, **61**, 129–134.
13. FUKUZAWA, S., HASHIMURA, T., SASAKI, M., YAMABE, H. and YOSHIDA, O., 1995. Nuclear morphometry for improved prediction of the prognosis of human bladder carcinoma. *Cancer*, **10** (76), 1790–1796.
14. LIPPONEN, P. K., ESKELINEN, M. J., KIVIRANTA, J. and NORDLING, S., 1991. Classic prognostic factors, flow cytometric data, nuclear morphometric variables and mitotic indexes as predictors in transitional cell bladder cancer. *Anticancer Research*, **11**, 911–916.
15. SOWTER, C., SLAVIN, G. and ROSEN, D., 1990, Morphometry of bladder carcinoma. Definition of a new variable. *Analytical Cellular Pathology*, **2**, 205–213.
16. DE PREZ, C., DE LAUNOIT, Y., KISS, R., PETEIN, M., PASTEELS, J., VERHEST, A. and VAN VELTHOVEN, R., 1990, Computerized morphonuclear cell image analyses of malignant disease in bladder tissues. *Journal of Urology*, **143**, 694–699.
17. FAUGERAS, O., and PRATT, W., 1980, Decorrelation methods of texture feature extraction. *IEEE Transactions on Pattern Analysis and Machine Intelligence*, PAMI-2, **14**, 323–332.
18. STREET, W. N., WOLBERG, W. H. and MANGASARIAN, O. L., 1993, Nuclear feature extraction for breast tumor diagnosis. *International Symposium on Electronic Imaging: Science and Technology*, San Jose, California, 1905, 861–870.
19. CONNERS, R. and HARLOW, C., 1980, A theoretical comparison of texture algorithms. *IEEE Transactions on Pattern Analysis and Machine Intelligence*, **3**, 204–222.
20. HARRALICK, R. and SHANMUGAM, K., 1973, Textural features for image classification. *IEEE Transactions on Systems, Man, and Cybernetics*, **3** (6), 610–621.
21. OHANIAN, P. and DUBES, R., 1992, Performance evaluation for four classes of textural features. *Pattern Recognition*, **8** (25), 819–833.
22. WALKER, R. F., JACKWAY, P. T. and LOVELL, B., 1995, Cervical cell classification via co-occurrence and Markov random field features. *Proceedings of Digital Image Computing: Techniques and Applications*, 294–299.
23. THEODORIDIS, S., and KOUTROUMBAS, K., 1998, Classifiers based on Bayes decision theory. In *Pattern Recognition*. (Academic Press), 13–28.
24. THEODORIDIS, S. and KOUTROUMBAS, K., 1998, Feature Subset Selection. In *Pattern Recognition*. (Academic Press), 159–160.
25. THEODORIDIS, S. and KOUTROUMBAS, K., 1998, System evaluation. In *Pattern Recognition*. (Academic Press), 342–343.
26. OOMS, E. C. M., ANDERSON, W. A. D., ALONS, C. L., BOON, M. E. and VELDHIJZEN, R. W., 1983, An analysis of the performance of pathologists in the grading of bladder tumors. *Human Pathology*, **14**, 140–143.
27. STENDAHL, U., WILLEN, H. and WILLEN, R., 1981, Invasive squamous cell carcinoma of the uterine cervix II: reproducibility of a histopathological malignancy system. *Acta Radiologica Oncology*, **20**, 65–70.
28. LANGLEY, F. A. and BAAK, J. P. A., 1984, Quantitative methods in diagnostic gynaecological pathology. *Clinical Obstetrics and Gynecology*, **11**, 79–92.
29. SCHAPERS, R. F. M., PLOEM-ZAAIJER, J. J., PAUWELS, R. P., SMEETS, N. B., BRANDT, P., TANKE, A. J., BOSMAN, F. T., 1993. Image cytometric analysis in transitional cell carcinoma of the bladder. *Cancer*, **72**, 182–189.
30. PREWITT, J. M. S., 1972, Objective characterization of tissue sections by digital image processing. *Proc of the 17th Annual Conference on Engineering in Medicine and Biology*, 481.
31. SOWTER, C., SLAVIN, G. and ROSEN, D., 1987, Morphometry of bladder carcinoma. The automatic delineation of urothelial nuclei in tissue sections using an IBAS II image array processor. *Journal of Pathology*, **153**, 289–297.
32. GONZALEZ, R. C. and WOODS, R. E., 1992, Recognition and interpretation. In *Digital Image Processing*. (Addison-Wesley), 580–581
33. DU BUF, J. M. H., KARDAN, M. and SPANN, M., 1990, Texture feature performance for image segmentation. *Pattern Recognition*, **3**, 291–309, 23.
34. GONZALEZ, R. C. and WOODS, R. E., 1992, Representation and description. In *Digital Image Processing*. (Addison-Wesley), 518–528.
35. WALKER, F. R., JACKWAY, P. and LONGSTAFF, I. D., 1995, Improving co-occurrence matrix feature discrimination. *Proceedings of DICTA '95, The 3rd Conference on Digital Image Computing: Techniques and Applications*, 643–648.

36. CHEN, P. C., and PAVLIDIS, T., PATRICK, C. C. and THEODOSIOS, P., 1979, Segmentation by texture using a co-occurrence matrix and a split-and-merge algorithm. *Computer Graphic and Image Processing*, **10**, 172-182.
37. KRUGER, P. R., THOMPSON, W. B. and TURNER, A. F., 1974, Computer diagnosis of pneumoconiosis. *IEEE Trans. Systems Man Cybernetics* SMC-4, 40-49.
38. <http://www.richland.cc.il.us/james/lecture/m170/ch07-clt.html>

## Appendix A

### Image segmentation

In isolating nuclei from the surrounding background tissue, a minimum distance classifier [32] was used, employing auto-correlation textural features [17]. The decision function of the classifier is of the form:

$$d_i(x) = x' m_i - \frac{1}{2} m_i' m_i, \quad i = 1, 2 \quad (\text{A1})$$

where  $x'$ : is the transposed feature vector; and  $m_i$ : is the mean feature vector for class  $i$ .

The minimum distance classification rule can be stated as:

If  $d_1(x) > d_2(x)$ ,  $x$  is classified to class 1.

If  $d_1(x) < d_2(x)$ ,  $x$  is classified to class 2.

Textural features were computed from:

$$S(u, v) = \sum_{m=0}^5 \sum_{n=-5}^5 (m - n_m)^u (n - n_n)^v A_F(m, n) \quad (\text{A2})$$

where,

$$n_m = \sum_{m=0}^5 \sum_{n=-5}^5 m A_F(m, n) \quad (\text{A3})$$

$$n_n = \sum_{m=0}^5 \sum_{n=-5}^5 n A_F(m, n) \quad (\text{A4})$$

In equations A2-A4, computation is only over one-half of the autocorrelation function because of its symmetry [17].

Finally,

$$A_F(m, n) = \sum_j \sum_k F(j, k) F(j - m, k - n) \quad (\text{A5})$$

is the auto-correlation function over a  $5 \times 5$  window.  $F$  is the function of the properly zero padded  $5 \times 5$  image sub-region.

Since texture is a region property [33], bigger windows capture better the context of texture but eliminate the accuracy of nuclei contours. A window size of  $5 \times 5$  was an optimum compromise between texture discrimination ability and nuclei boundary detection.

In the present study the cross-relation

$$S(1, 1) \sum_{m=0}^5 \sum_{n=-5}^5 (m - n_m)^1 (n - n_n)^1 A_F(m, n) \quad (\text{A6})$$

and the second-degree spread

$$S(2, 2) \sum_{m=0}^5 \sum_{n=-5}^5 (m - n_m)^2 (n - n_n)^2 A_F(m, n) \quad (\text{A7})$$

were evaluated.

In case of misclassification, an opening morphological operation was first applied to separate touching nuclei and to eliminate classification-noise, in the shape of small isolated structures. Additionally, small holes inside the nucleus area were filled by a closing operation. These morphological operations [34] are defined as combinations of fundamental operations, dilation and erosion, and can be written as follows:

$$\mathbf{O} (I_0, SE1) = \mathbf{D} (\mathbf{E} (I_0, SE1), SE1) \quad (\text{A8})$$

$$\mathbf{C} (I_0, SE2) = \mathbf{E} (\mathbf{D} (I_0, SE2), SE2) \quad (\text{A9})$$

where  $\mathbf{D}$  denotes the dilation operation,  $\mathbf{O}$  the open operation,  $\mathbf{E}$  the erosion operation, and  $\mathbf{C}$  the close operation.

$SE_1$  : is an octagonal structuring element  $11 \times 11$ .

$SE_2$  : is an octagonal structuring element  $7 \times 7$ .

The size of  $SE_1$  and  $SE_2$  was chosen as to effectively remove noisy regions and complete the internal of nuclei, without affecting significantly the details of nuclei shape.

In case of nucleus overlapping, the resulting structure was automatically eliminated by evaluating concavity (see Appendix B) and roundness and comparing them to corresponding pre-determined nuclei values. Roundness was evaluated by:

$$roundness = \frac{perimeter^2}{4 * \pi * area} \quad (\text{A10})$$

## Appendix B

### Best feature combination

Highest classification accuracy was obtained by the following four-feature combination: variance of nucleus intensity, correlation<sub>(d=1)</sub>, correlation<sub>(d=3)</sub>, standard deviation of concavity.

Variance: Assuming  $P(I)$  is the fraction of pixels with grey level  $I$ , and  $N_g$  the total number of possible grey levels.

$$\mu_2 = \sum_{I=0}^{N_g} (I - m)^2 * P(I) \quad (B1)$$

where  $m = \sum_{I=0}^{N_g} I * P(I)$  is the mean value. (B2)

Correlation: Texture feature of correlation estimated from the co-occurrence matrix [19–22]

$$P(i, j|d) = \frac{1}{4} * \sum_{\Phi=0,45,90,135} (P_i, j|d, \Phi) \quad (B3)$$

Each  $P(i, j|d, \Phi)$  is the probability of going from grey level  $i$  to grey level  $j$ , given that the inter-sample spacing is  $d$ , and the direction is given by angle  $\Phi$ .

The correlation was estimated as follows:

$$\text{Correlation} = \frac{\sum_{i=0}^{N_g-1} \sum_{j=0}^{N_g-1} (i - \mu_x)(j - \mu_y)P(i, j|d)}{\sigma_x \sigma_y} \quad (B4)$$

where:

$$\mu_x = \sum_{i=0}^{N_g-1} i \sum_{j=0}^{N_g-1} P(i, j|d), \quad (B5)$$

$$\mu_y = \sum_{j=0}^{N_g-1} j \sum_{i=0}^{N_g-1} P(i, j|d), \quad (B6)$$

$$\sigma_x^2 = \sum_{i=0}^{N_g-1} (i - \mu_x)^2 \sum_{j=0}^{N_g-1} P(i, j|d), \quad (B7)$$

$$\sigma_y^2 = \sum_{j=0}^{N_g-1} (j - \mu_y)^2 \sum_{i=0}^{N_g-1} P(i, j|d). \quad (B8)$$

$N_g$  is the number of grey scales.

Since each grey level is not efficiently employed to describe the picture, the co-occurrence matrix ( $N_g \times N_g$ ) should have many fewer entries than the total number of pixels in the image to avoid a sparse matrix [21]. A reasonable choice of  $N_g$  depends therefore on the application image size. To reduce the number of grey levels, each nuclear image is re-quantized to 16 levels ( $N_g = 16$ ) via histogram equalization, so that enough resolution kept to retain the texture of each nucleus, and  $N_g \times N_g$  is small enough compared to the total number of pixels in the nucleus.

This technique has been used by a number of research workers as an image preprocessing before texture features are computed from the co-occurrence matrices [35–37].

Finally, each co-occurrence feature was estimated for inter-sample spacing  $d = 1$  and  $d = 3$ , and four angles ( $\Phi = 0^\circ, 45^\circ, 90^\circ, 135^\circ$ ). For each inter-sample spacing we are averaging across the four angles equation (B3).

Concavity: This feature attempts to measure the severity of concavities or the indentations of a nucleus and was computed as follows:

Chords are drawn between non-adjacent contour points, and the ratio of the number of pixels lying inside the chords to the total number of pixels comprising the nucleus border was estimated. The chords joined contour points every twenty pixels and they moved in a circle every five pixels (figure B1).

It turned out that taking the features in groups of five did not improve the classification accuracy significantly. The best 5-dimensional feature vector gave 90.4% (57/63) accuracy for the low-risk cases, and 86.2% (25/29) accuracy for the high risk cases. The gain was one additional case classified correctly in the low-risk class.

To design a well-generalized classifier, we kept the minimum feature vector dimension beyond which no important gain in performance was obtained [24].

### Appendix C

The Bayes classifier is based on parametric methods, where gaussian distributed data is assumed. The gaussian model of features is a well-fitted model as far as the mean value of the nuclei features are concerned. According to the Central Limit Theorem the distribution of sample means should be approximately normal if the samples are large enough. Taking a sample of at least 30 nuclei, the sample distribution of the mean of a parameter (feature) will be approximately normal no matter the shape of the distribution of the individual values in the population [38].

Assuming that patterns  $\mathbf{x}$  follow the general multivariate normal density in the 4-dimensional feature space, the Bayes decision function is of the form [23]:

$$d_i(\mathbf{x}) = \log(P\omega_i) - \frac{1}{2} \log|C_i| - \frac{1}{2} [(\mathbf{x} - \mathbf{m}_i)' C_i^{-1} (\mathbf{x} - \mathbf{m}_i)]; \quad (C1)$$

$C_i$ :  $4 \times 4$  covariance matrix for class  $\omega_i$ ,

$$C_i = \frac{1}{N_i} \sum_{\mathbf{x} \in \omega_i} [\mathbf{x}\mathbf{x}' - \mathbf{m}_i \mathbf{m}_i'] \quad (C2)$$

$\mathbf{m}_i$ : the mean feature vector for each class  $\omega_i$ .

$\mathbf{x}'$ : the transposed feature vector.

$P\omega_i$ : The a priori probability estimated from the available training patterns.

Assuming  $N$  the total number of feature vectors and  $N_i$  of them belonging to  $\omega_i$ , then  $P\omega_i \approx \frac{N_i}{N}$ . In our case the a priori probability for the low-risk class was  $P\omega_1 = \frac{63}{92}$ , and the a priori probability for the high-risk class was  $P\omega_2 = \frac{29}{92}$ .